

## EFFECT OF IMPURITIES ON BENDING FATIGUE STRENGTH OF STRUCTURAL STEEL

Tomasz Lipinski, Anna Wach

University of Warmia and Mazury in Olsztyn, Poland  
tomekl@uwm.edu.pl, anna.wach@uwm.edu.pl

**Abstract.** Non-metallic inclusions as impurities found in steel can affect its performance characteristics. Their impact depends not only on their quality, but also, among others, on their size and distribution in the steel volume. The literature mainly describes the results of tests on hard steels. The article discusses the results of a study investigating the effect of the number of submicroscopic non-metallic inclusions (up to 2  $\mu\text{m}$  in size) on the fatigue strength of structural steel during rotary bending. The study was performed on 21 heats produced in an industrial plant. Fourteen heats were produced in 140 t electric furnaces, and 7 heats were performed in a 100 ton oxygen converter. All heats were desulfurized. Seven heats from electrical furnaces were refined with argon, and heats from the converter were subjected to vacuum circulation degassing. The experimental variants were compared in view of the applied melting technology and heat treatment options. The fatigue strength of steel with impurity spaces was determined during rotary bending. The results revealed that the fatigue strength is determined by the impurity spaces and tempering temperature.

**Keywords:** steel, structural steel, fatigue strength, bending fatigue, impurities, non-metallic inclusions.

### Introduction

Commercial iron alloys apart of typical chemical elements contain sulfur, oxygen, and those elements form solutions in liquid metal. The physical and chemical reactions that occur in the process of steel melting and solidification produce non-metallic compounds and phases, referred to as inclusions. The quantity of non-metallic inclusions is correlated with the content of admixtures in the alloy, while their phase composition and structure, in particular shape, dimensions and dispersion, are determined by the course of metallurgical processes. The distribution of non-metallic inclusions in steel and their quality are determined by various factors, including charge quality, process regime, furnace type and out-of-furnace processing [1-6].

Fatigue degradation is a type of damage that occurs over time and causes significant losses. Fatigue strength of agricultural machine parts is a particularly important factor in their reliability. These machines operate on an uneven surface. Thus, the agricultural machine parts are more likely to variable load than parts of other machines. According to Kocańda and other researches, non-metallic inclusions larger than 5  $\mu\text{m}$  may affect the fatigue strength of steel [1; 3; 7].

Fatigue occurs and develops gradually due to cyclic service load that causes stress. Initial stages are marked by the incubation of slips the number of which increases in individual grains. When critical values are exceeded, the material cracks and becomes fit for scrap [8-11].

The combined effect of internal microstresses resulting from the presence of non-metallic inclusions in steel and stress caused by external load plays an important role in the formation and development of fatigue cracks. Internal stress is a function of the morphological composition of impurities, but it is most affected by the heat processing environment [3]. The above is inclusive of the thermal expansion of structural components under the influence of heat. The role of non-metallic inclusions in steel is determined not only by their quality, distribution or size, but also by the quality of steel and the type of load applied to the final product during use. The impact of non-metallic inclusions on steel properties begins in microareas, and it spreads to macroscopic steel. Inclusions are generally regarded as negative phenomena, but their role has not yet been fully explained [1; 11-13].

Structural steels with a medium carbon content operating at changing loads are also widely used in industry. Mining chains are an example of their use. Despite the important role played by these steels, the number of conducted studies analyzing impurities found in them is much higher for hard steels [3; 7; 8]. This probably results from a more detailed analysis of this problem. Nevertheless, the acting mechanism of a non-metallic inclusion located in a plastic matrix differs from the analogous mechanism for a rigid matrix. This observation is also an inducement to take up this subject of research.

The developed models for analyzing the effect of impurities spaces on the set mechanical parameters of analogous steels can be used to simulate these features on condition. This justifies the need to conduct research on this subject. Since the impurities spaces are determined by the course of the metallurgical process, this study set out to test materials produced with the involvement of various methods.

### Materials and methods

The objective of this study was to determine the influence of submicroscopic impurities space (up to 2  $\mu\text{m}$  in size of impurity) on the bending fatigue strength of structural steel with medium carbon contents.

The tested material comprised steel manufactured in three different metallurgical processes: in an arc furnace with two out-side treatments variant and a converter with deoxidized. The resulting heats differed in purity and size of non-metallic inclusions. Heat treatments were selected to produce heats with different microstructure of steel, from hard microstructure of tempered martensite, through sorbitol to the ductile microstructure of spheroidite.

The experimental material consisted of steel products obtained in three metallurgical processes. In the first process, steel was melted in a 140-ton basic arc furnace. The study was performed on 21 heats produced in an industrial plant. The metal was tapped into a ladle, it was desulfurized and 7-ton ingots were uphill teemed. Billets with a square section of 100x100 mm were rolled with the use of conventional methods. As part of the second procedure, steel was also melted in a 140-ton basic arc furnace. After tapping into a ladle, steel was additionally refined with argon. Gas was introduced through a porous brick, and the procedure was completed in 8-10 minutes. Steel was poured into moulds, and billets were rolled similarly as in the first method. In the third process, steel was melted in a 100-ton oxygen converter and deoxidized by vacuum. Steel was cast continuously and square 100x100 mm billets were rolled. Billet samples were collected to determine:

- chemical composition. The content of alloy constituents was estimated with the use of LECO analyzers, an AFL FICA 31000 quantometer and conventional analytical methods;
- relative volume of non-metallic inclusions with the use of the extraction method,
- dimensions of impurities by inspecting metallographic specimens with the use of a Quantimet 720 video inspection microscope under 400x magnification. It was determined for a larger boundary value of 2  $\mu\text{m}$ .

The number of particle range 2  $\mu\text{m}$  and smaller was the difference between the number of all inclusions determined by chemical extraction and the number of inclusions measured by the video method.

Analytical calculations were performed on the assumption that the quotient of the number of particles on the surface divided by the area of that surface was equal to the quotient of the number of particles in volume divided by that volume [14].

With the aim of qualification of fatigue proprieties from every melting 51 sections were taken. The sections had the shapes of a cylinder about diameter 10 mm. Their main axis can be directed to the direction of plastic processing simultaneously. It thermal processing was subjected it was with the aim of differentiation of building of structural sample [14]. It depended on hardening from austenitizing by 30 minutes in temperature 880 °C after which it had followed quenching in water, for what drawing was applied. Tempering depended on warming material for 120 minutes in temperature 200, 300, 400, 500 or 600 °C and cooling down on air.

Fatigue strength was determined for all heats. Heat treatment was applied to evaluate the effect of hardening on the fatigue properties of the analyzed material, subject to the volume of fine non-metallic inclusions. During heat treatment, steel sections were hardened and tempered at temperature of 200, 300, 400, 500 and 600 °C. The application of various heat treatment parameters led to the formation of different microstructures responsible for steel hardness values in the following range from 271 to 457 HV.

Examination was implemented on calling out to a rotary curving machine at the frequency of pendulum cycles: 6000 periods on minute. For the basis of fatigue defining the endurance level

10<sup>7</sup> cycles was accepted. The level of fatigue-inducing load was adapted to the strength properties of steel. Maximum load was set at:

- for steel tempered at a temperature of 200 °C – 650 MPa,
- for steel tempered at a temperature of 300-500 °C – 600 MPa,
- for steel tempered at a temperature of 600 °C – 540 MPa.

During the test, the applied load was gradually reduced in steps of 40 MPa (to support the determinations within the endurance limit). Load values were selected to produce 10<sup>4</sup>-10<sup>6</sup> cycles characterizing the endurance limits [7].

The general form of the mathematical model is presented by equation (1)

$$z_{go \text{ (temp. tempered)}} = a\lambda + b, \tag{1}$$

where  $z_{go}$  – rotating bending fatigue strength, MPa  
 $\lambda$  – impurities space,  $\mu\text{m}$ ,  
 $a, b$  – coefficients of the equation.

The significance of correlation coefficients  $r$  was determined on the basis of the critical value of the Student’s  $t$ -distribution for a significance level  $\alpha = 0.05$  and the number of degrees of freedom  $f = n-2$  by formula (2).

$$t = \frac{r}{\sqrt{\frac{1-r^2}{n-2}}}. \tag{2}$$

The values of the diffusion coefficient  $z_{go}$  near the regression line were calculated with the use of the below formula (3):

$$\delta = 2s_{z_{go}}\sqrt{1-r^2}, \tag{3}$$

where  $s_{z_{go}}$  – standard deviation ,  
 $r$  – correlation coefficient.

**Results and discussion**

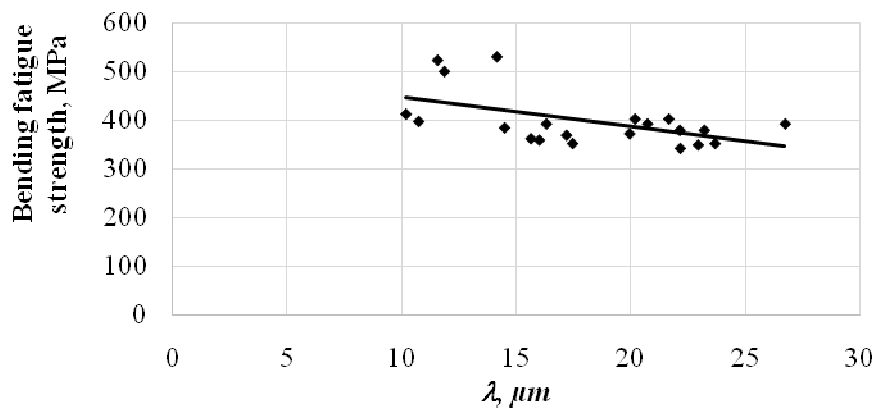
The average chemical composition of the analyzed steel is presented in Table 1.

Table 1

**Average chemical composition of the analyzed steel**

C	Mn	Si	P	S	Cr	Ni	Mo	Cu	B
0.24	1.19	0.25	0.02	0.013	0.51	0.49	0,24	0.11	0.003

The bending fatigue strength of steel hardened and tempered at 200 °C depending on the impurities space is presented in Fig. 1, regression equation and correlation coefficients  $r$  at (4).



**Fig. 1. Bending fatigue strength of steel hardened and tempered at 200 °C subject to impurities space**

$$z_{go(200)} = -6.048\lambda + 507.16 \text{ and } r = 0.5362, \quad (4)$$

where  $r$  – correlation coefficient.

For the impurities space  $\lambda = 10 \mu\text{m}$  the bending fatigue strength is about 450 MPa. With the increase of the impurities space to  $27 \mu\text{m}$ , the bending fatigue strength decreased to about 350 MPa.

The bending fatigue strength of steel hardened and tempered at  $300^\circ\text{C}$  depending on the impurities space is presented in Fig. 2, regression equation and correlation coefficients  $r$  at (5).

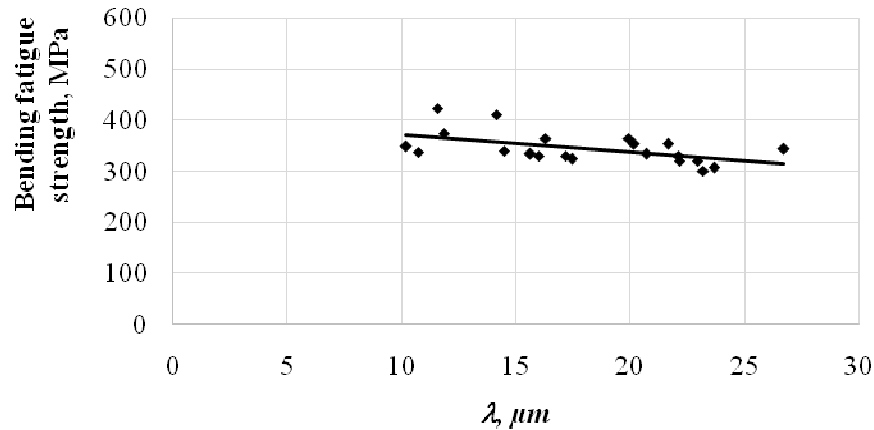


Fig. 2. Bending fatigue strength of steel hardened and tempered at  $300^\circ\text{C}$  subject to impurities space

$$z_{go(500)} = -3.3402\lambda + 404.55 \text{ and } r = 0.5288. \quad (5)$$

The bending fatigue strength of steel hardened and tempered at  $400^\circ\text{C}$  depending on the impurities space is presented in Fig. 3, regression equation and correlation coefficients  $r$  at (6).

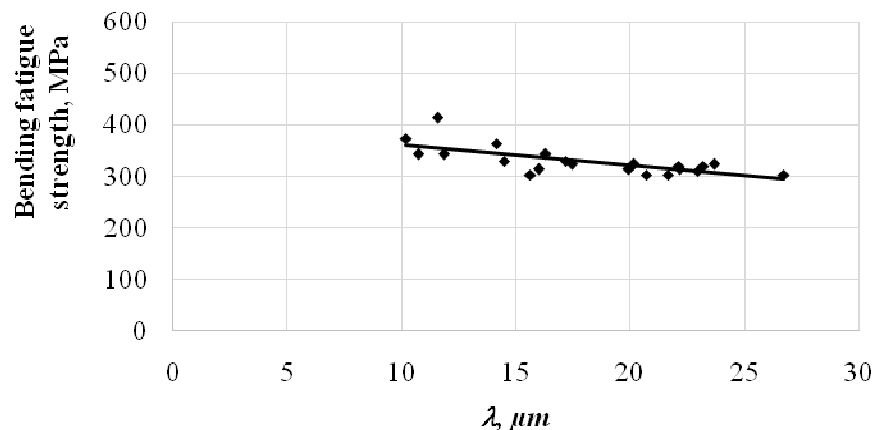


Fig. 3. Bending fatigue strength of steel hardened and tempered at  $400^\circ\text{C}$  subject to impurities space

$$z_{go(300)} = -4.0502\lambda + 402.02 \text{ and } r = 0.7104. \quad (6)$$

No significant differences were noted in the bending fatigue strength at tempering temperatures of  $300^\circ\text{C}$  (Fig. 2) and  $400^\circ\text{C}$  (Fig. 3).

The bending fatigue strength of steel hardened and tempered at  $500^\circ\text{C}$  depending on the impurities space is presented in Fig. 4, regression equation and correlation coefficients  $r$  at (7).

$$z_{go(600)} = -2.9123\lambda + 344.07 \text{ and } r = 0.6103. \quad (7)$$

The bending fatigue strength of steel hardened and tempered at  $600^\circ\text{C}$  depending on the impurities space is presented in Fig. 5, regression equation and correlation coefficients  $r$  at (8).

$$z_{go(400)} = -2.2125\lambda + 294.96 \text{ and } r = 0.4677. \quad (8)$$

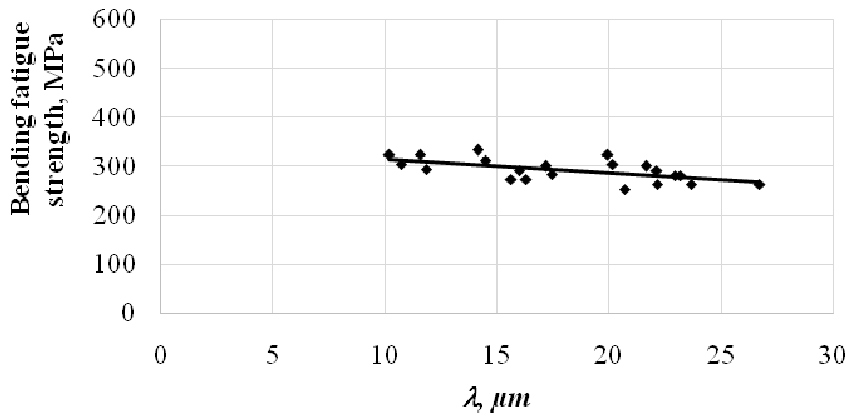


Fig. 4. Bending fatigue strength of steel hardened and tempered at 500 °C subject to impurities space

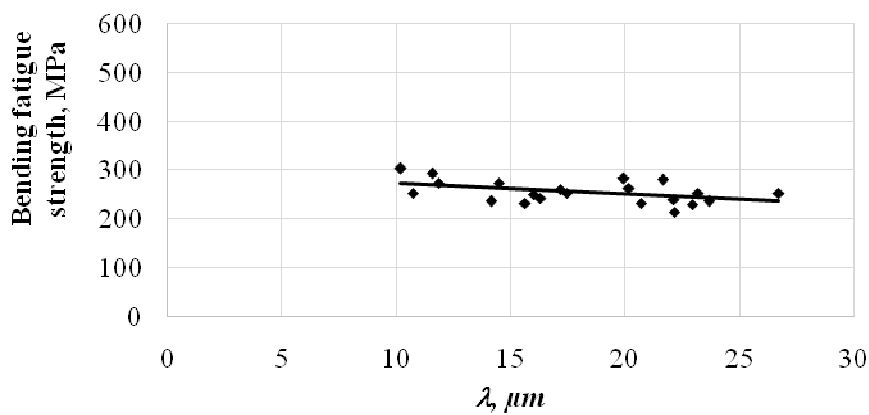


Fig. 5. Bending fatigue strength of steel hardened and tempered at 600 °C subject to impurities space

The principal structure of steel is identical for the remaining two main production methods with respective heat treatment variants. The parameters representing mathematical models and correlation coefficients are presented in Table 2.

Table 2

Parameters representing mathematical models and correlation coefficients

Tempering temperature °C	Regression coefficient <i>a</i> (1)	Regression coefficient <i>b</i> (1)	Correlation coefficient <i>r</i>	Degree of dissipation $z_{go}$ around regression line $\delta$ , MPa (3)	$t_{\alpha=0.05}$ calculated by (2)	$t_{\alpha=0.05}$ from Student's distribution for $p = (n-2)$
200	-6.048	507.16	0.5362	91.16	2.769	2.093
300	-3.3402	404.55	0.5288	38.70	2.716	
400	-4.0502	402.02	0.7104	42.23	4.400	
500	-2.9123	344.07	0.6103	36.12	3.358	
600	-2.2125	294.96	0.4677	47.73	2.307	

The analysis of coefficients *a* and *b* (Tab. 2) in regression equations (1) indicates that fatigue strength (parameter *b*) decreases with a rise. The effect of impurities space (parameter *a*) decreases, too but for 300 °C as a tempering temperature the effect is high. Parameter *a* decreases with increasing plasticity steel matrix, which is possible with increased tempering temperature. It can be

assumed that at low tempering temperatures, long impurities spaces further contribute to the brittleness of tempered martensite.

In the analyzed tempering temperature (Fig. 1-6), the lowest bending fatigue strength was noted for the top tempering temperature, this means 600 °C. In contrast, the highest bending fatigue strength was noted for the lowest tempering temperature, this means 200 °C. Increasing the tempering temperature causes a change from the hard steel microstructure tempering of martensite on plastic spheroidite, consequently decreasing the fatigue strength. Generally, for all tempering temperatures, with increasing impurities space  $\lambda$  bending fatigue strength decreases.

### Conclusions

1. The results of the study indicate that the fatigue strength, represented by the fatigue strength during rotary bending, is correlated with the impurities space. The presence of statistically significant correlations was verified by the Student's *t*-test.
2. Higher tempering temperature causes smaller dispersion of values around the regression line.
3. The results of the study indicate that the bending fatigue strength increases as the impurities space decreases.

### References

1. Lipiński T., Wach A., Dimensional Structure of Non-Metallic Inclusions in High-Grade Medium Carbon Steel Melted in an Electric Furnace and Subjected to Desulfurization. *Solid State Phenomena* 223, 2015, pp. 46-53.
2. Himemiya T., Wołczyński W., Prediction of Solidification Path and Solute Redistribution of an Iron-based Multi-component Alloy Considering Solute Diffusion in the Solid Materials. *Transactions of the Japan Institute of Metals* 43, 2002, pp. 2890-2896.
3. Murakami Y., Kodama S., Konuma S., Quantitative evaluation of effects of non-metallic inclusions on fatigue strength of high strength steels, I: basic fatigue mechanism and fatigue fracture stress and the size and location of non-metallic inclusions, *Int J Fatigue* 11(5), 1989, pp. 291-298.
4. Park J. S., Park J. H., Effect of Slag Composition on the Concentration of Al<sub>2</sub>O<sub>3</sub> in the Inclusions in Si-Mn-killed Steel. *Metallurgical and Materials Transactions B* 45B, 2014, pp. 953-960.
5. Lipiński T., Wach A., Influence of Outside Furnace Treatment on Purity Medium Carbon Steel. 23<sup>rd</sup> International Conference on Metallurgy and Materials Metal 2014 Brno TANGER Ltd., Ostrava. Conference proceedings 2014 pp. 738-743.
6. Gulyakov V. S., Vusikhis A. S., Kudinov D. Z., Nonmetallic Oxide Inclusions and Oxygen in the Vacuum Jet Refining of Steel. *Steel in Translation* 42 (11), 2012, pp. 781-783.
7. Kocańda S., Zmęczyeniowe pękanie metali (Metal fatigue cracking). WNT Warszawa 1985 (in Polish).
8. Zhang J.M., Zhang J.F., Yang Z.G., Li G.Y., Yao G., Li S.X., Hui W.J., Weng Y.Q., Estimation of maximum inclusion size and fatigue strength in high-strength ADF1 steel. *Material. Science and Engineering A* 394, 2005, pp. 126-131.
9. Lipiński T., Wach A., The Effect of Fine Non-Metallic Inclusions on The Fatigue Strength of Structural Steel. *Archives of Metallurgy and Materials* 60 (1), 2015, pp. 65-69.
10. Chapetti MD, Tagawa T, Miyata T., Ultra-long cycle fatigue of high-strength carbon steels. Part II: estimation of fatigue limit for failure from internal inclusions. *Material Science Engineering A* 356, 2003, pp. 236-244.
11. Roiko A., Hänninen H., Vuorikari H., Anisotropic distribution of non-metallic inclusions in a forged steel roll and its influence on fatigue limit, *International J. of Fatigue* 41, 2012, pp. 158-167.
12. Murakami Y., *Metal fatigue. Effects of small defects and inclusions.* Elsevier 2002.
13. Srivastava A., Ponson L., Osovski S., Bouchaud E., Tvergaard V., Needleman A., Effect of inclusion density on ductile fracture toughness and roughness. *Journal of the Mechanics and Physics of Solids* 63, 2014, pp. 62-79.
14. Ryś J., *Stereologia materiałów (Stereology of materials).* Fotobit Design, Kraków 1995 (in Polish).